GEOLOGIJA *65/2*, 149–158, Ljubljana 2022
https://doi.org/10.5474/geologija.2022.009

Prediction of the peak shear strength of the rock joints with artificial neural networks

Napoved vrhunske strižne trdnosti po razpoki v kamnini z nevronskimi mrežami

Karmen FIFER BIZJAK & Rok VEZOČNIK

Slovenian National Building and Civil Engineering Institute, Dimičeva ul. 12, SI-1000 Ljubljana, Slovenia;
e-mail: karmen.fifer@zag.si, rok.vezocnik@zag.si

Prejeto / Received 4. 5. 2022; Sprejeto / Accepted 7. 10. 2022; Objavljeno na spletu / Published online 18. 11. 2022

Key words: artificial neural network, camera-type 3D scanner, rock mechanics, rock joint, joint roughness
Ključne besede: nevronska mreža, 3D skener s kamero, mehanika kamnin, razpoke, hrapavost razpok

Abstract

With the development of computer technology, artificial neural networks are becoming increasingly useful in the field of engineering geology and geotechnics. With artificial neural networks, the geomechanical properties of rocks or their behaviour could be predicted under different stress conditions. Slope failures or underground excavations in rocks mostly occurred through joints, which are essential for the stability of geotechnical structures. This is why the peak shear strength of a rock joint is the most important parameter for a rock mass stability. Testing of the shear characteristics of joints is often time consuming and suitable specimens for testing are difficult to obtain during the research phase. The roughness of the joint surface, tensile strength and vertical load have a great influence on the peak shear strength of the rock joint. In the presented paper, the surface roughness of joints was measured with a photogrammetric scanner, and the peak shear strength was determined by the Robertson direct shear test. Based on six input characteristics of the rock joints, the artificial neural network, using a backpropagation learning algorithm, successfully learned to predict the peak shear strength of the rock joint. The trained artificial neural network predicted the peak shear strength for similar lithological and geological conditions with average estimation error of 6 %. The results of the calculation with artificial neural networks were compared with the Grasselli experimental model, which showed a higher error in comparison with the artificial neural network model.

Izvleček

Nevronske mreže postajajo z razvojem računalniške tehnologije vedno bolj uporabne tudi na področju inženirske geologije in geotehnike. Z nevronskimi mrežami lahko na osnovi večjega števila podatkov napovemo geomehanske lastnosti kamnine ali njihovo obnašanje v različnih napetostnih pogojih. Porušitve brežin ali podzemnih prostorov v kamninskem masivu se večinoma pojavijo po razpokah, zato so strižne lastnosti v razpokah ali prelomih bistvene za stabilnost geotehničnih objektov. Preiskave strižnih lastnosti so večinoma dolgotrajne, prav tako pa je pri vrtanju v fazi raziskav težko pridobiti primerne vzorce. Velik vpliv na velikost vrhunske strižne trdnosti ima hrapavost površine razpoke, natezna trdnost in vertikalna obremenitev. V predstavljenem članku je hrapavost površine razpok izmerjena s fotogravimetričnim skenerjem, vrhunska strižna trdnost pa je določena z Robertsonovo direktno strižno preiskavo. Na osnovi šestih vhodni karakteristik razpok in kamnine ter izmerjene strižne trdnosti z Robertsonovo preiskavo, lahko z naučeno nevronsko mrežo uspešno napovemo vrhunsko strižno trdnost po razpoki. Tako naučena nevronska mreža lahko dovolj natančno napove vrhunsko strižno trdnost za podobne litološke razmere in geološke pogoje, z upoštevanjem dokaj nizke napake, to je 6 %. Rezultate izračuna z nevronskimi mrežami smo primerjali z eksperimentalnim modelom, ki je v primerjavi z nevronskimi mrežami pokazal višjo napako napovedi vrhunske strižne trdnosti.

Introduction

The idea for artificial neural networks (ANN) is in the functioning of the human brain. The human brain is the central system of the human nervous system, composed from almost 10 billion biological neurons that are interconnected by synapses. The cellular body of a neuron receives input signals from many synapses with different electrical activity (Flood & Kartam, 1994, Bishop, 1995, Lopez et. al., 2022).

Scientists were therefore drawn to the idea of making a device that mimics the brain. These are made up of a huge number of cells interconnected by thin "threads". These cells are called neurons, and their connections or "threads" are called synapses. Neurons send electrical stimuli to each other through synapses. Synapses are characterized by differences in electrical conductivity, which changes during learning. Thus, the knowledge acquired during learning is accumulated in synapses or in their conductivity. If the sum of the signals arriving at an individual neuron via synapses is large enough, the ignition of an individual neuron occurs. This means that this neuron sends a signal to its output, which is transmitted through the synapses to other neurons (Jain et al., 1996, Maio & Santillo, 2020).

The ANN tries to simulate the human brain activity and until now several applications are already known in rock mechanics field (Lawal & Kwon, 2021; Abdalla et al., 2015; Armaghani, 2015; Hussain et al., 2019; Sarkar et al., 2010).

The shear behaviour of a jointed rock masses depends on the shear characteristics of the discontinuities in the rock mass. To determine the shear strength in rock mass discontinuities many researchers developed experimental relationships between the roughness of the discontinuities and the peak shear strength (Barton, 1973; 1976; Barton and Choubey, 1977; Hoek and Brown, 1980; Hoek and Bray, 1981; Hoek, 2000; Huang et al., 1992; Patton, 1966; Pellet et al., 2013).

Recently, scanners have been used as a non-destructive method to measure and characterise the joint surface in three dimensions. The roughness metric based on the three-dimensional morphology was proposed by Grasselli (2001, 2002). An ATOS scanner was used for the accurate measurement of the joint roughness. Details of the scanner characteristics are summarized in Table 1. Several empirical relations were developed for determining the geometry of the joint surface, such as contact area A^0, roughness parameter C and maximum dip angle Θ^*_{max} (Grasselli & Egger, 2003).

ANNs have already been used for prediction of the shear characteristics of rock samples in published papers. The shear strength of shale rock samples was predicted based on the minimum and intermediate strength using a triaxial test (Moshrefi et al., 2018). Back propagation multi-layer perceptron was used for learning. Influence of heterogeneity on rock strength at different strain rates was predicted with an ANN, as well as parameters of crack inclination, distance, filling and strain rate (Jiang et al., 2021). Shear behaviour of clean rock discontinuities was studied including normal stress, dilation, horizontal displacement, asperity angle, amplitude, joint rock compressive strength and friction angle of an intact sample. The ANN model fitted the measuring results better than some analytical models. Shear strength parameters were obtained using shale samples, sheared in a triaxial cell. The input parameters were point load index, Brazilian tensile strength, ultrasonic velocity, Schmidt hammer test and friction angle as an output parameter (Armaghani et al., 2014).

Drilling data and well logs were used for the uniaxial compressive strength prediction with ANN (Asadi, 2017). Porosity, density, penetration rate and P wave velocity were used to predict the uniaxial strength of rock between wells that are close to each other. For limestone the uniaxial strength was compared with the results of the ANN and regression analysis (Khanlari & Abdilor, 2011).

Table 1. Characteristics of the scanner with camera (ATOS I).
Tabela 1. 3D skener s kamero (ATOS I).

Item	Value
Measured Points	800.000
Measurement Time (seconds)	0.8
Measuring Area (mm²)	125 ×100 - 1000 × 800
Point Spacing (mm)	0.13-1.00
Measuring volume (mm³)	125 × 100 × 90 to 1000 × 800 × 800
Measuring points per individual scan	1032 × 776 pixels

In the presented paper, the ANN was used for the peak shear strength prediction of the rock joints. The input parameters were tensile strength, basic shear angle and the morphologic parameters of the rock joints obtained from the 3D scanner measurements. Results were compared with the Robertson direct shear test for different rock samples.

Methods

Artificial Neural network model

The model of the ANN tries to simulate the behaviour of the human brain and nervous system by its architecture. A detailed description of the ANNs is beyond the scope of this paper and can be found in many publications (Masters, 1993; Jain et al., 1996; Almeida, 2002; Shahin et al., 2002).

ANNs learn from the presented data and use these data to adjust their weights in an attempt minimise the model input variables and the corresponding outputs. The advantage of ANNs is that they do not need any prior knowledge about the relationship between the input-output variables. This is a benefit in comparison with most of the empirical and statistical methods.

The basic unit of ANN is a neuron or node (Fig. 1). It receives input signals (x_1 .. x_n) and a bias value, which is always 1. In the neuron input, signals are multiplied with their weight values (w_1 .. w_n). The bias assures that even if all input signals are zero, there is activation in the neuron. The activation function ($G_{(I)}$) is used for introducing the non-linearity to the ANN.

$$I = w_0 + w_1 y_1 + w_2 y_2 \ldots . + w_n y_n \qquad (1)$$

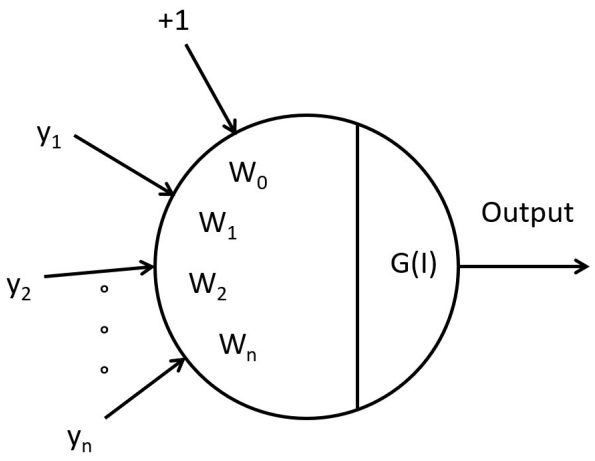

Fig. 1. Typical neuron in ANN.
Sl. 1. Značilen nevron v ANN.

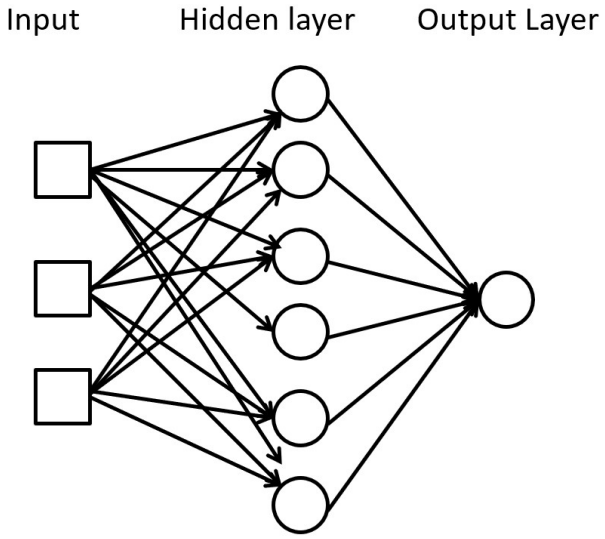

Fig. 2. Structure of the BP artificial neural network.
Sl. 2. Struktura povratne nevronske mreže.

A typical ANN is composed of three different layers of neurons; one input layer, one or multiple hidden layers and one output layer. The simplified model is presented in Figure 2.

The input layer consists of neurons which receive information from input data. The number of neurons in the input layer depends on input data sources. For presented application the input neurons were; σ_t (tensile strength), φ_b (basic friction angle) and scanning parameters A_0 (maximum contact area), C (roughness parameter) and θ_{max}* (maximum apparent dip angle).

The hidden layer contains a different number of neurons and is connected with the input and output layer with a linear or non-linear transfer function (Rashidian et al., 2013). The hidden layer processes the information received from the input neurons, and passes it to the output layer.

The output layer produces an appropriate response to the given input. For presented ANN there is a single output neuron; measured shear peak shear stress (τ_p).

The propagation of information in ANNs starts at the input layer where the network is presented with a historical set of input data and the corresponding (desired) outputs. The back-propagation algorithm, used in this paper, is the most widespread because it has a simple structure and clear mathematical meaning (Cybenko, 1989). It consists of two phases: forward and backward. In the forward phase, the training data set was introduced to the network and fed forward until a prediction was calculated. The final output is then compared to the target value and the error signal is calculated. In the backward phase, the error signal is back propagated in the network from the output layer to the input layer and the

appropriate weight changes are calculated using a mathematical criterion that minimizes the errors (Jain et al., 1996; Khandelwal et al., 2004).

Using these errors and a learning rule, the network adjusts its weights until it can find a set of weights that calculate an input/output pair with the smallest error. This phase is called "learning" or "training". Once the training phase of the model has been successfully finished, the performance of the trained model has to be validated using an independent validation set of data.

For the presented application 70 % of the data were used for a training set and the rest for the testing. The test set measured how well the model learned based on the data from the learning phase. For validation, data are usually taken from the whole set when there are not enough additional data for this procedure.

Use of a 3D Scanner

For measuring rock joint surface roughness, an Advanced Topometric Sensor (ATOS I) was used (Fig. 3) which operates by combining measuring principles of optical triangulation, photogrammetry and fringe projection (Keller & Mendricky, 2015). With the help of a projector, different light-dark fringe patterns are produced by the measuring part.

The ATOS system consists of three separate components: the fringe digital projector and two CCD cameras. The two cameras, separated by a fixed distance, operate on the basis of known relative orientation thus forming the basis for triangulation. The fringe digital projector, located midway between both cameras, projects a structured light pattern onto the object to be scanned. During the scanning process, the coded fringe pattern undergoes a phase shift which means the pattern rapidly changes and is therefore nearly invisible to the human visual perception abilities. This pattern alteration process is recorded by the two CCD sensors with 3D coordinates calculated for each camera pixel by applying optical transformation equations. The resulting highly-detailed image consists of millions of measuring 3D points which are acquired within a very short time (few seconds) without physically contacting the scanned surface. In the final step, the accompanying sensor software automatically generates a high-resolution point cloud which represents a precise 3D image of the scanned surface. Optionally, this point cloud can be further transformed into a surface model (using typical triangular or square grid templates (Fig. 4). In the figure the roughness of the rock joint surface measured from the share plane is presented.

The quality of surface measurements is obviously very important for the estimation of surface roughness. The quality of the morphological model depends on the density of the measuring points, the measuring resolution and the precision with which these points can be located in space. The measuring area of the ATOS I system ranges from 125 × 100 mm^2 to 1000 × 800 mm^2 and the number of measuring points per individual scan reaching up to 1032 × 776 pixels.

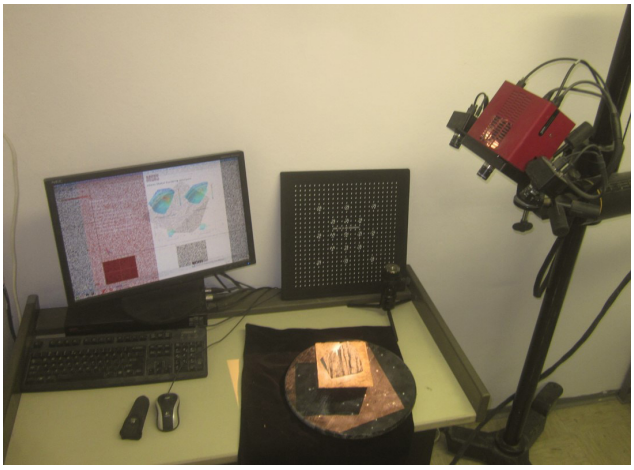

Fig. 3. The ATOS I 3D scanner and the sample.
Sl. 3. Skener ATOS I 3D in skenirani vzorec.

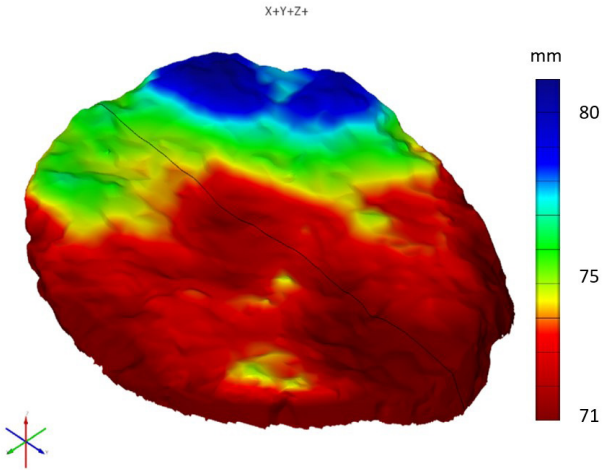

Fig. 4. Surface model of the rock joint.
Sl. 4. Skenirana površina razpoke.

Calculation methods of Grasselli model for the peak shear stress calculation

Morphological parameters were calculated from scanning samples according to the Grasselli (2001) procedure (G01). The apparent dip angle was used to calculate the three-dimensional morphology parameters (Fig. 5). The procedure is presented in equations 2 to 6.

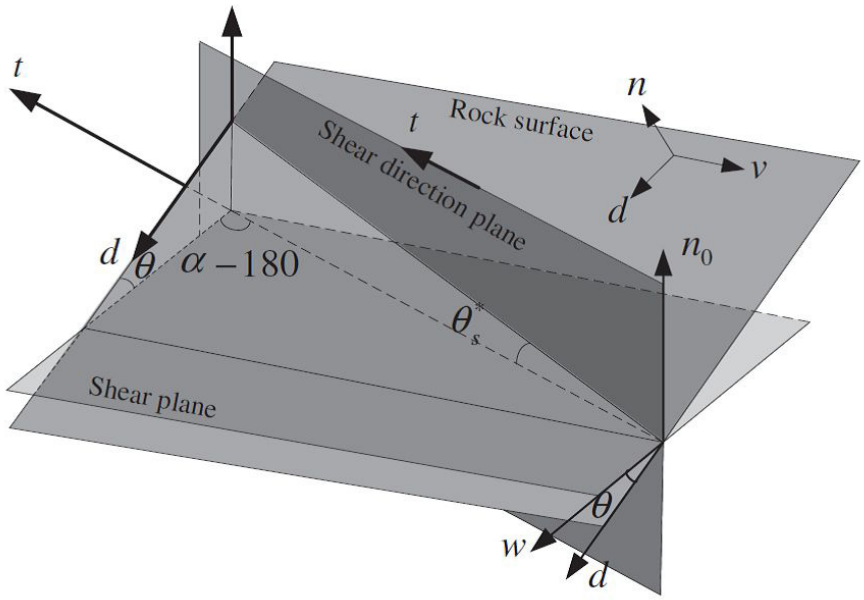

Fig. 5. Geometrical identification of apparent dip angle - θ^*.

Sl. 5. Geometrična predstavitev navideznega kota - θ^*.

$$\tan\theta_s^* = \tan\theta\,(-\cos\alpha) \quad (2)$$

$$\cos\theta = \frac{nn_o}{|n||n_o|} \quad (3)$$

$$\cos\alpha = \frac{tn_1}{|t||n_1|} \quad (4)$$

$$\overline{\theta^*} = \frac{tn_1}{|t||n_1|}\frac{1}{m}\sum_{i=1}^{m}\theta_{si}^* \quad (5)$$

where m is the number of triangles, θ^* is the apparent dip angle of the surface unit, α is the azimuth, θ is the dip angle between the shear plane and the joint surface, t is the shear direction vector, n is the outward normal vector of the triangle, n_0 is the outward normal vector of the plane and n_1 is the projection vector of n. The maximum contact area (A_0) is calculated as follows:

$$A_0 = \frac{A_l}{A_m} \quad (6)$$

Where A_m is the area of the rock joint and A_l the contact area after the shear test.

The results from the ANN and from the Grasselli procedure were used for comparison. The peak shear strength of the samples was calculated according to the proposed criteria (Grasselli, 2001) according to the eq. 7.

$$\tau_p = \sigma_n * tan(\varphi_r') * \left(1 + exp\left(-\frac{1}{9A_0} * \frac{\theta_{max}^*}{C} * \frac{\sigma_n}{\sigma_t}\right)\right) \quad (7)$$

where σ_n is the normal stress, σ_t is tensile strength of the rock, φ_r basic angle of friction, θ^*_{max} is the maximum apparent dip angle of the surface unit, C is the roughness parameter, calculated using a best-fit regression function, which characterises the distribution of the apparent dip angles over the surface. Brazilian tests were done for tensile strength of the rock samples.

An average estimation error (E_{ave}) was calculated (Kulatilake et al., 1995) for both results (ANN and Grasselli model).

$$E_{ave} = \frac{1}{m}\sum_{i=1}^{m}\left|\frac{\tau_{test}-\tau_{cal.}}{\tau_{test}}\right| * 100\% \quad (8)$$

Test procedure

Samples of different lithology were taken from the north part of Slovenia for a direct shear Robertson test. Samples had a diameter of less than 10 cm and had a natural rock joint. They were tested under different vertical stress between 0.1 and 0.4 MPa. Robertson direct shear tests were performed according to the ASTM D5607 -16 standards and the final result of these tests was peak shear strength for every sample (τ_p). A shear test of basic friction angle was performed in a shear apparatus for every lithological type of rock (φ_r). Before the capsulation of the samples, the joints of the samples were scanned with the ATOS I scanner to obtain the morphological parameters. A data processing program, written in MatLab, was developed for the calculation of the rock joint morphological parameters according to Grasselli (2001).

Results

The morphological parameters of the rock joints (A_0, C, θ^*_{max}) were calculated as a result of scanning. The rest of the input parameters; σ_n, σ_t, and φ_b, were obtained from the Robertson direct shear test. The morphological parameters and shear strength parameters are presented in Table 2.

Table 2. Input data for the peak shear strength calculation
Tabela 2. Vhodni podatki za izračun vrhunske strižne trdnosti

No	Lithology	σ_t (MPa)	σ_n (MPa)	A_0 (-)	C (-)	Θ^*_{max} (°)	ϕ_b (°)
1	limestone	1.99	0.1	0.4147	17.03	86.86	24
2	limestone	1.99	0.3	0.5791	16.99	89.69	24
3	limestone	1.99	0.4	0.5499	28.75	75.55	24
4	limestone	1.99	0.4	0.1773	12.87	86.2	24
5	limestone	1.99	0.4	0.4859	20.87	82.807	24
6	limestone	1.99	0.3	0.4015	11.82	89.86	24
7	limestone	1.99	0.2	0.3953	27.92	86.95	24
8	limestone	1.99	0.4	0.4535	12.2	51.89	24
9	dolomite	2.17	0.15	0.3410	11.9	90	25
0	shale	0.3	0.4	0.5420	15.04	86.21	24
11	shale	0.3	0.2	0.4720	9.22	42.93	24
12	siltstone	2	0.1	0.4606	6.26	73.33	26
13	siltstone	2	0.4	0.2000	11.61	87.28	26
14	siltstone	2	0.4	0.3037	13.88	89.12	26
15	claystone	0.3	0.2	0.1200	19.98	84.74	20
16	claystone	0.3	0.2	0.4707	24.69	87.1	20
17	claystone	0.3	0.1	0.3459	13.27	89.9	20
18	sandstone	1	0.4	0.4613	11	79.25	30
19	claystone	0.3	0.1	0.4999	6.69	89.7	20
20	claystone	0.3	0.4	0.5020	9.4	84.24	24
21	siltstone /claystone	1	0.4	0.3655	28.62	89.9	24
22	claystone	0.3	0.4	0.3953	24.4	79.72	24
23	siltstone/ claystone	0.3	0.2	0.5105	9.25	89.05	24
24	siltstone	7.37	0.4	0.4238	15.05	89.71	30
25	dolomite	3.02	0.1	0.5829	6.46	79.12	30
26	dolomite	3.02	0.3	0.4821	7.21	82.08	30
27	siltstone	2	0.3	0.5153	12.46	84.87	30
28	dolomite	3.02	0.3	0.4821	7.21	82.09	30
29	dolomite	2.49	0.25	0.4126	6.06	90	28
30	claystone	0.3	0.4	0.4824	15.59	85.47	20

The prediction of peak shear stress (τ_p) with ANN and G01 model was performed in the next step. For both calculations the same input parameters were used (σ_n, σ_t, A_0, C, θ^*_{max}, φ_b).

Results of the ANN model

Several ANN structures were used for the τ_p prediction, with a different number of neurons in the input layer, but the best results were achieved with the next structure:

Input layer; 6 neurons (σ_n, σ_t, A_0, C, θ^*_{max}, φ_b)
Hidden layer, 29 neurons
Output layer, one neuron (τ_p)

For example, if we added residual shear angle (φ_r) and type of lithology to the presented 6 input neurons, the calculation made by the ANN did not converge to the minimum error.

A hyperbolic tangent transfer function was used as the activation function. We also used an sigmoidal function, but the average estimation error (E_{av}) was almost the same. The trained ANN predicted the peak shear strength with quite a small average estimation error; E_{av} = 6 % (Table 2). A comparison between the predicted peak shear strength with the ANN and with the results from the laboratory Robertson test is presented in Figure 6.

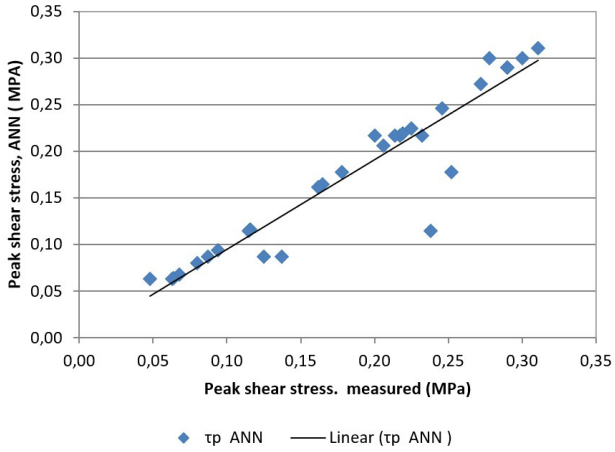

Fig. 6. Measured peak shear stress vs ANN predicted.
Sl. 6. Primerjava izmerjene vrhunske strižne trdnosti in izračunane z ANN.

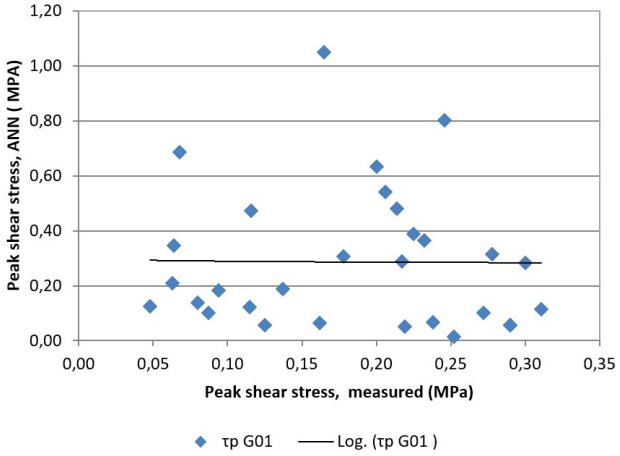

Fig. 7. Measured peak shear stress vs G01 model.
Sl. 7. Primerjava izmerjene vrhunske strižne trdnosti in izračunane z G01 modelom.

Result of G01 model

Next calculation was done based on the G01 model (eq. 8) and compared with the results obtained from laboratory Robertson tests. The average estimation error between the Robertson tests and calculation with G01 model was much higher, E_{av} = 28 % (Table 3).

The comparison between the calculated peak shear strength with the G01 model and with the results from the laboratory Robertson test is presented in Figure 7.

Table 3. Results of peak shear strength calculation for ANN and G01 model.
Tabela 3. Rezultati izračuna vrhunske strižne trdnosti izračunani z ABB in G01 modelom.

No	τ_p meas. (MPa)	τ_p ANN (MPa)	τ_p G01 (MPa)	No	τ_p meas. (MPa)	τ_p ANN (MPa)	τ_p G01 (MPa)
1	0.06	0.06	0.35	16	0.07	0.07	0.68
2	0.25	0.18	0.01	17	0.05	0.06	0.13
3	0.17	0.17	1.05	18	0.31	0.31	0.11
4	0.21	0.21	0.54	19	0.06	0.06	0.21
5	0.20	0.22	0.63	20	0.28	0.30	0.31
6	0.18	0.18	0.31	21	0.27	0.27	0.10
7	0.12	0.12	0.47	22	0.22	0.22	0.05
8	0.23	0.22	0.36	23	0.14	0.09	0.19
9	0.12	0.12	0.12	24	0.25	0.25	0.80
0	0.30	0.30	0.28	25	0.09	0.09	0.18
11	0.13	0.09	0.06	26	0.29	0.29	0.06
12	0.08	0.08	0.14	27	0.23	0.23	0.39
13	0.22	0.22	0.29	28	0.29	0.29	0.06
14	0.21	0.22	0.48	29	0.24	0.12	0.07
15	0.09	0.09	0.10	30	0.16	0.16	0.07
					E_{ave}	6%	28%

Discussion

The presented calculation was demonstrated by analysing 30 samples of jointed rock. The input parameters for the Grasselli calculation (G01) and the ANN were the same. The peak shear stress depends on the normal stress under which the shear test is performed and because of this, the normal stress (σ_n) is one of the most important parameters. Grasseli (2001) showed that A_0, C and θ^*_{max}, are the most important morphological parameters and tensile strength (σ_t) and basic friction angle ϕ_b are the most important strength characteristics of the rock.

The peak shear stress of the rock joints was measured in laboratory and then predicted with the ANN and with the G01 model. The results of both calculations are presented in Figure 8. Prediction of peak shear stress with the ANN is very close to the measured results, while the calculations with the Grasselli model were much higher in comparison to the measured results for at least for 30 % of samples.

Samples used in a comparable study (Grasselli, 2001) have larger dimensions, at least 200 mm × 100 mm × 100 mm and were consolidated under a normal load higher than 1 MPa. In our case, samples were tested under the normal loads between 0.1 and 0.4 MPa. The use of smaller samples and lower vertical load are probably a reason for the higher average estimation error obtained with the G01 model. Such large samples are often difficult to obtain for testing. Samples are usually taken from boreholes and they have a maximal diameter of 10 cm and in this case the Robertson shear test is much more convenient. The result of the Robertson test was peak shear stress which was then calculated with the ANN and Grasselli model.

The calculation with the ANN reaches very good results; E_{ave} was 6 %. The calculated Pearson coefficient was 0.93, which confirms a very high correlation between the measured peak shear stress and the predicted peak shear stress with ANN. The comparison between the calculated and measured peak shear strength is presented in Figure 8.

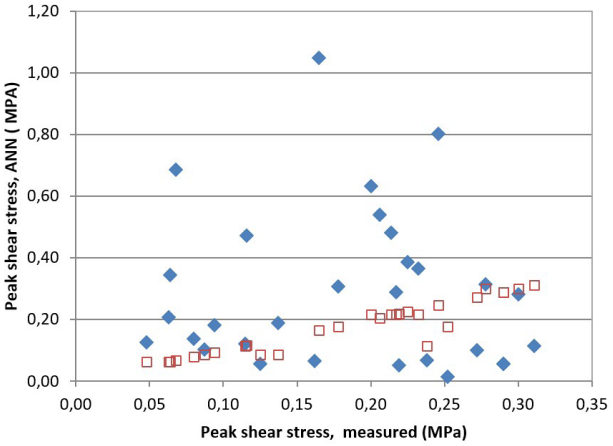

Fig. 8. Peak shear stress; measured, predicted with ANN and calculated with G01 model.

Sl. 3. Vrhunska strižna trdnost, napovedana z ANN in izračunana z G01.

Results of more tests with different rock lithology have to be included in to the ANN in the future. Given the diverse lithological composition in Slovenia, it is necessary to include samples of metamorphic and igneous rocks. Also, the number of samples of soft rock has to be increased, because the main geotechnical problems usually occurred in soft rocks like shale or claystone.

Higher number of samples could assure that the trained ANN would be a useful tool in engineering practice.

Conclusions

Shear geomechanical characteristic are the most important factor in the stability of the jointed rock mass. Usually the failure occurs along a fissure or a joint. Peak shear stress is the main parameter for a slope design, foundations or tunnel excavations. If it is exceeded, the failure could cause large damage to geotechnical structures. In the paper the technology of rock joint scanning was used for determining the morphological parameters of the joint roughness. Additional parameters were obtained from the Robertson direct shear test and tensile strength from the Brazilian test. Results showed that the ANN could successfully predict the peak shear with quite small error. The future research will be focused on analysing more samples with different lithology, especially soft rock, to make the ANN usable for wider engineering practice.

References

Abdalla J.A., Attom M.F. & Hawileh R. 2015: Prediction of minimum factor of safety against slope failure in clayey soils using artificial neural network. Environmental Earth Science, 73/9: 5463–5477. https://doi.org/10.1007/s12665-014-3800-x

Ak, H. & Konuk, A. 2008: The effect of discontinuity frequency on ground vibrations produced from bench blasting: a case study. Soil Dynamics and Earthquake Engineering, 28/9: 686–694. https://doi.org/10.1016/j.soildyn.2007.11.006

Almeida, J.S. 2002: Predictive non-linear modeling of complex data by artificial neural networks. Current Opinion in Biotechnology, 13/1: 72–76. https://doi.org/10.1016/s0958-1669(02)00288-4

ASTM – 16 2017: Standard Test Method for Performing Laboratory Direct Shear Strength Tests of Rock Specimens Under Constant Normal Force. ASTM International.

Asadi, A. 2017: Application of artificial neural networks and prediction of uniaxial compressive strength of rock usinf well logs and drilling data. Procedia Engineering 191: 279–286. https://doi.org/10.1016/j.proeng.2017.05.182

Armaghani, D.J., Hajihassani M., Bejarbaneh B., Y., Marto A. & Mohamad, E.T. 2014: Indirect measure of shale shear strength parameters by means of rock index tests through an optimised artificial neural network. Meassurement, 55: 487–498.

Armaghani, J.D., Momeni E., Khalil, A.S. & Khandelwal, M. 2015: Feasibility of ANFIS model for prediction of ground vibrations resulting from quarry blasting. Environmental Earth Sciences, 74: 2845–2860. https://doi.org/10.1007/s12665-015-4305-y

Barton, N. 1973: Review of a new shear-strength criterion for rock joints. Eng. Geol., 7/4: 287–332. https://doi.org/10.1016/0013-7952(73)90013-6

Barton, N. 1976: The shear strength of rock and rock joints. Int. J. Rock. Mech. and Min. Sci. & Geomech. Abstr., 13/97: 255–279. https://doi.org/10.1016/0148-9062(76)90003-6

Barton, N. & Choubey, V. 1977: The shear strength of rock joints in theory and practice. Rock Mechanics, 10:1–54. https://doi.org/10.1007/BF01261801

Bishop, C.M. 1995: Neural network for pattern recognition (1st ed). Oxford University Press.

Cybenko, G. 1989. Approximation by superpositions of a sigmoidal function. Math. Control Signals Systems, 2: 303-314. https://doi.org/10.1007/BF02551274

Flood, I. & Kartam, N. 1994. Neural networks in civil engineering. I: principles and understanding. Journal of Computing in Civil Engineering, 8/2: 131-148.

Grasselli, G. 2001: Shear strength of rock joints based on quantified surface description. (Dissertation). Ecole Polytechnique Federale de Lausanne, Lausanne.

Grasselli, G., Wirth, J. & Egger, P. 2002: Quantitative three-dimensional description of a rough surface and parameter evolution with shearing. International Journal of Rock Mechanics and Mining Sciences, 39: 789–800.

Grasselli, G. & Egger, P. 2003: Constitutive law for the shear strength of rock joints based on three-dimensional surface parameters. International Journal of Rock Mechanics and Mining Sciences, 40: 25–40.

Hoek, E. & Bray, J. W. 1981: Rock slope engineering. Vancouver, CRC Press.

Hoek, E. & Brown, E. T. 1980: Empirical strength criterion for rock masses. Journal of Geotechnical and Geoenvironmental Engineering, 106: 1013–1035.

Hoek, E. 2000: Shear strength of discontinuities. Rock engineering, 61–72. https://www.rocscience.com/assets/resources/learning/hoek/Practical-Rock-Engineering-Full-Text.pdf

Huang, S. L., Oelfke, S. M. & Speck, R. C. 1992: Applicability of fractal characterization and modelling to rock joint profiles. International Journal of Rock Mechanics and Mining Sciences & Geomechanics Abstracts, 29: 89–98.

Hussain, A., Surendar, A., Clementking, A., Kanagarajan, S. & Ilyashenko, L.K. 2019: Rock brittleness prediction through two optimization algorithms namely particle swarm optimization and imperialism competitive algorithm. Engineering with Computers, 35/3: 1027–1035. https://doi.org/10.1007/s00366-018-0648-9

Jain, A.K., Mao, J. & Mohiuddin, K.M. 1996: Artificial neural networks - a tutorial. Computer, 29/3: 31–44.

Jiang S., Sharafisasafa, M. & Shen, L. 2021: Using Artificial neural networks to predict influence of heterogeneity on rock strength at different strane raits. Materials, 14/11: 3042. https://doi.org/10.3390/ma14113042

Keller, P. & Mendricky, R. 2015: Parameters influencing the precision of slm production. MM Science Journal, October 2015.

Khanlari, G. & Abdilor, Y. 2011: Estimation odf strength parameters of limestone using artificial neural network and regression analysis. Australian Journal of basic and Applied Science, 5/11: 1049–1053.

Kulatilake, P. H. S. W., Shou, G., Huang, T. H. & Morgan, R. M. 1995: New peak shear strength criteria for anisotropic rock joints. International Journal of Rock Mechanics and Mining Sciences & Geomechanics Abstracts, 32/7: 673–697.

Khandelwal, M., Roy, M.P. & Singh, P.K. 2004: Application of artificial neural network in mining industry. Indian Mining Engineering Journal, 43: 19-23.

Lawal, A.I. & Kwon, S. 2021: Application of artificial intelligence to rock mechanics: An overview. Journal of Rock Mechanics and Geotechnical Engineering, 13/1: 248-266.

Lopez, O.A.M., Lopez, A.M. & Crossa, J. 2022: Fundamentals of Artificial Neural Networks and Deep Learning. Multivariate Statistical Machine Learning Methods for Genomic Prediction: 379–425. Springer, Cham. https://doi.org/10.1007/978-3-030-89010-0_10

Maio, V.D. & Santillo, S. 2020: Information Processing and Synaptic Transmission. Advances in Neural Signal Processing. https://doi.org/10.5772/intechopen.88405

Masters, T. 1993: Practical network recipes in C++. Academic Press, San Diego, California, USA.

Moshrefi, S., Shahriar, K., Ramezanzadeh, A. & Goshtasbi, K. 2018: Prediction of ultimate strength of shale using artificial neural network. Journal of mining & Environment, 9/1: 91–105. https://doi.org/10.22044/jme.2017.5790.1390

Patton, F.D. 1966: Multiple modes of shear failure in rock. In: Proceedings of the 1st congress of International Society for Rock Mechanics, 1: 509–513.

Pellet, F. L., Keshavarz, M. & Boulon, M. 2013: Influence of humidity conditions on shear strength of clay rock discontinuities. Engineering Geology, 157: 33–38.

Rashidian, V. & Hassanlourad, M. 2013: Application of Artificial Neural Network for Modeling the Mechanical Behavior of Carbonate Soils. International Journal of Geomechanics, (ASCE) GM.1943-5622.0000299.

Sarkar, K., Tiwary, A. & Singh, T.N. 2010: Estimation of strength parameters of rock using artificial neural networks. Bulletin of Engineering Geology and the Environment, 69: 599–606.

Shahin, M.A., Jaksa, M.B. & Maier H.R. 2001: Artificial neural network-based Settlement Prediction Formula for Shallow Foundations on Granular Soils, Australian Geomechanics.